Vol. 89: 75–86, 2023 https://doi.org/10.3354/ame01998

AQUATIC MICROBIAL ECOLOGY Aquat Microb Ecol

Published online June 15





Quorum sensing signal disrupts viral infection dynamics in the coccolithophore *Emiliania huxleyi*

Elizabeth L. Harvey¹, Han Yang², Emma Castiblanco², Megan Coolahan², Genevieve Dallmeyer-Drennen², Naomi Fukuda², Eleanor Greene², Marley Gonsalves¹, Sara Smith¹, Kristen E. Whalen^{2,*}

¹Department of Biological Sciences, University of New Hampshire, Durham, NH 03824, USA ²Biology Department, Haverford College, Haverford, PA 19041, USA

ABSTRACT: Viruses that infect phytoplankton are abundant in all regions of the global ocean. Despite their ubiquity, little is understood regarding how biotic interactions can alter virus infection success as well as the fate of phytoplankton hosts. In previous work, the bacterially derived compound 2-heptyl-4-quinolone (HHQ) has been shown to protect the cosmopolitan coccolithophore *Emiliania huxleyi* from virus-induced mortality. The present study explores the potential mechanisms through which protection is conferred. Using a suite of transmission electron microscopy and physiological diagnostic staining techniques, we show that when *E. huxleyi* is exposed to HHQ, viruses can gain entry into cells but viral replication and release is inhibited. These findings are supported by a smaller burst size, as well as lower infectious and total virus production when the host is treated with nanomolar concentrations of HHQ. Additionally, diagnostic staining results indicate that programmed cell death markers commonly associated with viral infection are not activated when infected *E. huxleyi* are exposed to HHQ. Together, these results suggest that the ability of HHQ to inhibit infectious viral production protects the alga not from getting infected, but from cell lysis. This work identifies a new mechanistic role of bacterial quorum sensing molecules in mediating viral infections in marine microbial systems.

KEY WORDS: Phytoplankton · Bacteria · HHQ · Microbial interactions · Viral infection

1. INTRODUCTION

Viruses are the most numerous biological entities in the marine environment at 10^{30} in total abundance and account for approximately 10^{23} infections every second (Suttle 2005). Representing a major source of mortality, viruses lyse approximately 20% of the oceanic photosynthetic biomass daily, influencing the composition of marine communities and oceanic biogeochemical cycles (Suttle 2007). One well-known host–virus pairing exists between the cosmopolitan coccolithophore *Emiliania huxleyi* (Prymnesiophyceae, Haptophyta) and its host-specific giant nucleocytoplasmic double-stranded DNA (dsDNA) *Cocco-*

lithovirus (E. huxleyi virus [EhV]) within the family *Phycodnaviridae* (Bratbak et al. 1993, Wilson et al. 2002). Annual blooms of *E. huxleyi* cover thousands of square kilometers of ocean surfaces (Holligan et al. 1993, Paasche 2001) and are routinely terminated by coccolithoviruses, resulting in both the cycling of nutrients within the microbial loop as well as the production of large aggregates that facilitate carbon export (Laber et al. 2018). Given the fundamental role of *E. huxleyi* in the oceanic carbon cycle, in both atmospheric CO_2 uptake leading to primary production (up to 20% of total fixed marine carbon) and CO_3^{-2} removal via calcification (Zondervan et al. 2002, Read et al. 2013), understanding factors that

© The authors 2023. Open Access under Creative Commons by Attribution Licence. Use, distribution and reproduction are unrestricted. Authors and original publication must be credited.

Publisher: Inter-Research · www.int-res.com

govern infection dynamics and virus-induced mortality will help better parameterize carbon export modeling efforts.

To date, significant research efforts have focused on abiotic factors that influence the success of viral infection of E. huxleyi, such as temperature (Kendrick et al. 2014), light (Thamatrakoln et al. 2019), and nutrient concentration (Jacquet et al. 2002). Similarly, biotic influences such as host density (Knowles et al. 2020), host ploidy level (Frada et al. 2017), and pro-viral signal-containing extracellular vesicles (Schatz et al. 2021) have also been shown to modulate host-virus dynamics. Most recently, small molecule chemical messengers secreted by host-associated microbes have been found to mediate infection dynamics (Pollara et al. 2021). For example, the bacterial quorum sensing signal 2-heptyl-4-quinolone (HHQ), previously established for its role in bacterial communication, allows E. huxleyi to evade virusinduced cell lysis (Pollara et al. 2021). While these findings present the first of its kind evidence that bacteria are capable of directly interfering with viral lysis of algal hosts, questions remain as to the mechanisms triggered by HHQ that allow the algal host to evade virus-induced mortality.

Insights gained from both a metabolomic (Rosenwasser et al. 2014) and molecular (Ku et al. 2020, Zhang et al. 2022) dissection of viral infection have revealed the complexity of the co-evolutionary 'arms race' between E. huxleyi and EhV (Bidle & Vardi 2011). Infection by EhVs rapidly remodels the host's metabolic network, redirecting resources to viralderived lipid biosynthesis (Rosenwasser et al. 2014), accompanied by the shutdown of host genes and the active expression of viral genes (Ku et al. 2020). Availability of host-supplied resources such as nucleotides is critical in early infection, as within 2 h postinfection (hpi), viral genes involved in DNA replication and nucleotide metabolism are transcribed (Ku et al. 2020). Over the course of infection, there is a concerted orchestration of viral gene transcription patterns whose seemingly all-or-none switch in activity and temporal sequence progression may be a viral strategy to optimize replication (Ku et al. 2020), suggesting events early in the viral transcriptional trajectory are critical for host hijacking. This infection window of crucial transitions between host and viral gene expression patterning is on the order of 2-8 hpi and parallels exactly the temporal cessation of cell cycle progression in HHQ-exposed E. huxleyi cells as evidenced by halted DNA replication (Pollara et al. 2021). Since viral infection and HHQ treatment remodel the ultrastructure and metabolic landscape of algal host cells on overlapping timescales upon onset of their application, HHQderived protection may thwart key mechanistic waypoints tied to early viral-host infection dynamics. Indeed, a 24 h delay of HHQ application to infected cultures does not rescue cells from viral-mediated demise (Pollara et al. 2021), indicating that HHQ must trigger an immediate response in the eukaryotic host to avoid death. Therefore, there are 2 primary mechanisms by which HHQ may protect E. huxleyi from viral lysis. Firstly, HHQ-induced reprogramming of host cellular architecture may interfere with the fundamental cellular processes exploited by the virus to gain entry into the alga. Alternatively, HHQ-induced physiological alterations may prevent the replication, proliferation, or release of the virus once infected. Delineating between these 2 potential mechanisms is essential for modeling this multikingdom interaction and would provide a framework for how bacterial chemical messengers may be able to manipulate viral success in the ocean.

Here, we elucidate the concentration of HHQ necessary for protection against viral mortality and demonstrate that HHQ is sufficient to protect the host alga regardless of viral strain or titer. We then provide evidence that HHQ-mediated protection is not the result of direct interaction between the alkylquinolone with the virus; rather, HHQ induces a time-dependent physiological change in the host necessary for protection. While HHQ does not prevent viral entry into host cells, the signal does inhibit viral replication, viral release, and the production of infectious virions compared to control cells. Given that lytic viral infection is dependent on the subsequent induction of host programmed cell death (PCD), which is triggered by the production of reactive nitrogen and oxygen species (NO and ROS, respectively) and concomitant activation of metacaspase activity, we examined diagnostic fluorescent assays to measure indicators of cell stress and PCD in HHQ-treated infected cultures. We provide evidence that viruses infecting HHQ-treated cultures are segregated into endo-lysosomal compartments and, therefore, are not able to tightly control the host's PCD machinery, likely leading to the observed loss of EhV production and significantly lower burst size compared to control cultures. In sum, this work adds a rich new layer of complexity to the E. huxleyi-EhV story by presenting evidence that chemical signaling by bacteria is capable of directly interfering with viral replication/release and algal host PCD trajectory, which has implications for understanding viral susceptibility in microbial-algal symbioses.

2. MATERIALS AND METHODS

2.1. General cultivation conditions

Unless otherwise noted, all experiments were conducted with axenic *Emiliania huxleyi* (CCMP2090, non-lith forming; National Center for Marine Algae and Microbiota). Algal cultures were grown in 0.2 µm filtered, autoclaved seawater with f/2 nutrients added minus silica (Guillard 1975). Cultures were maintained on a 14 h light (80 µmol photons m⁻² s⁻¹): 10 h dark cycle at 18°C, with a salinity of 35. These conditions are referred to hereafter as general culturing conditions. Strain purity was confirmed using f/2 MM and f/2 MB purity test broths and visually confirmed by epifluorescence microscopy with DAPI to detect bacterial contamination. Cultures were transferred weekly to maintain exponential growth.

The EhV strains used in this study (EhV 86 and EhV 201) were previously isolated from *E. huxleyi* blooms in the English Channel (Wilson et al. 2002, Nissimov et al. 2012) and were obtained from the laboratory of Dr. Kay Bidle, Rutgers University, New Brunswick, NJ, USA. Virus strains were propagated in exponentially growing cultures of *E. huxleyi*, as previously described (Bidle et al. 2007). Briefly, upon lysis of *E. huxleyi*, viral lysates were filtered through a 0.45 or 0.8 µm syringe filter to remove cell debris and stored in the dark at 4°C until used for subsequent infection experiments. In experiments with viral lysates, lysates were used within 1 wk of filtration.

2.2. Cell enumeration

Cells of *E. huxleyi* were enumerated using a flow cytometer (Guava, EasyCyte HT or BGHT) with species-specific settings, including forward scatter, side scatter, and red fluorescence (695/50 nm) emission characteristics for evaluating chlorophyll intensity. All samples were run live at $0.24~\mu l s^{-1}$ for 3~min.

To enumerate the total viruses in a culture, undiluted samples were fixed at 1% glutaraldehyde (sterile filtered), diluted between 1:10 and 1:100 with filtered sterile seawater or 1× phosphate-buffered saline (PBS), stained with 1× SYBR Green, incubated for 10 min on a heat block at 80°C in the dark, and then enumerated using the flow cytometer (Jacquet et al. 2002). Media-only (f/2-Si) blanks were processed in parallel to correct for background noise. To enumerate infectious (or active) virus, the most probable number assay (MPN) was used (Jarvis et al. 2010). For each MPN, aliquots from the experiment were

serially diluted 10 times in a stepwise fashion using a 10-fold dilution at each step. A 20 µl aliquot from each dilution or undiluted sample was dispensed into 6 replicate wells of a 96-well plate. To each well, 180 µl of axenic, exponentially growing E. huxleyi CCMP2090 was added. Wells containing 200 µl of E. huxleyi 2090 without virus addition served as the controls. The plates were incubated under general culturing conditions for 72 h before being read either by a SpectraMax M2e or via the flow cytometer for chlorophyll fluorescence as a proxy for cell abundance. Clearance (denoting infection and subsequent cell lysis) observed in wells on the plate was compared with control wells containing no virus, and MPN was calculated using the US Environmental Protection Agency's MPN calculator (https:// mostprobablenumbercalculator.epa.gov/mpnForm) with a Cornish-Fisher limit of approximation type.

2.3. Experimental design

Several experiments using the general culturing and enumeration conditions detailed above were conducted to test E. huxleyi's susceptibility to viral infection and mortality when exposed to HHQ. First, an experiment was conducted to examine the dose of HHQ that elicited complete viral protection as indicated by lack of cell loss post-infection. Prior to these experiments, EhV concentration in a stock of viral lysate was enumerated using flow cytometry to allow for dilution to a specific virus:host ratio in each experiment. Exponential cultures of E. huxleyi at 1×10^5 cells ml⁻¹ were exposed to EhV 201 (1:1 virus:host ratio), concurrently with a final concentration of either 1, 10, or 100 ng ml⁻¹ HHQ or a volumetric equivalent of DMSO in triplicate (never exceeding 0.2% v/v). Previous work has demonstrated no significant difference in E. huxleyi growth in the presence of the final concentrations of DMSO used in these experiments (Harvey et al. 2016, Pollara et al. 2021). Cultures were sampled daily for E. huxleyi cell abundance.

Second, the impact of HHQ-mediated protection of E. huxleyi cells in relation to EhV strain and virus:host ratios was examined. Triplicate exponential E. huxleyi cultures at 1×10^5 cells ml^{-1} were exposed to either EhV 201 or EhV 86 lysate at either 1:1 or 8:1 virus:host ratio, along with 100 ng ml^{-1} HHQ. Treatments with volumetric equivalent concentrations of DMSO served as controls. E. huxleyi cell abundance was monitored on the flow cytometer up to 120 hpi.

To examine the impact of pre-treating the virus with HHQ, viral lysates from 2 strains (EhV 201 and EhV 86) were either treated with 100 ng ml $^{-1}$ HHQ or a volumetric equivalent of DMSO for 96 h in duration. Following viral lysate pre-treatment, triplicate exponential *E. huxleyi* cultures at 1×10^5 cells ml $^{-1}$ were exposed to the pre-treated viral lysate (1:1 virus:host ratio). All treatments were monitored for 120 hpi for *E. huxleyi* cell abundance and total viral abundance.

2.4. Transmission electron microscopy and ultrastructure analysis

Exponentially growing E. huxleyi cultures at 1×10^5 cells ml⁻¹ were simultaneously dosed with EhV 201 (at an 8:1 virus:host ratio) and either 100 ng ml⁻¹ HHQ or a volumetric equivalent of DMSO. Cultures were incubated under general culture conditions, and 40 ml from all treatments were sampled every 24 h for E. huxleyi cell abundance and transmission electron microscopy (TEM) analysis over 96 hpi.

Cells were prepared for TEM analysis by concentrating 40 ml of culture on a 0.4 μm , 25 mm polycarbonate filter to 2 ml, then washing 3 times with 0.2 M sodium cacodylate buffer, pH 7.2, and resuspending concentrated cells in 2 ml of 0.2 M sodium cacodylate buffer. Cells were fixed in 1 ml aliquots in 2.5% glutaraldehyde in 0.2 M sodium cacodylate buffer, pH 7.2, and kept at 4°C in the dark. Both 1 ml fixed duplicate samples were combined and further concentrated on a 0.45 μm Corning SpinX (non-sterile) cellulose acetate column into a single sample with a final volume ranging from 190-220 µl. Samples were kept in the dark at 4°C and transported to the Electron Microscopy Resource Laboratory at the University of Pennsylvania for processing. Briefly, cells were postfixed in 2% osmium tetroxide for 1 h at room temperature and rinsed in double-distilled H₂O prior to en bloc staining with 2% uranyl acetate. After dehydration through a graded ethanol series, the cells were infiltrated and embedded in Embed-812 (Electron Microscopy Sciences). Thin sections were stained with uranyl acetate and lead citrate and examined with either the JEOL 1010 electron microscope fitted with a Hamamatsu digital camera and AMT Advantage NanoSprint500 software or a JEOL JEM-1400 electron microscope fitted with Gatan CCD camera and Gatan Digital Micrograph (version 1.83.842) and TEM Center for JEM-1400 software (version 1.3.4.2698).

To detect the underlying ultrastructural impacts of HHQ on E. huxleyi-EhV infection dynamics, the morphology of E. huxleyi cells was examined at the single cell level using the National Institutes of Health ImageJ software with Fiji built-in software tools (Schindelin et al. 2012). Approximately 30 cells per treatment were randomly selected for analysis at 24, 48, and 72 hpi; cells at 96 hpi were not analyzed due to a large extent of viral degradation in control samples. Cells were assessed for the number of virions per cell and morphological parameters previously described as indicative of EhV infection, including the percentage of cells with membrane blebbing, compromised membranes, and observable lipid bodies (Mackinder et al. 2009, Schatz et al. 2014, Liu et al. 2018).

2.5. Infection assays for diagnostic fluorescent assays

In triplicate, 500 ml polycarbonate bottles containing E. huxleyi cultures at a concentration of 1×10^5 cells ml^{-1} were inoculated with an 8:1 virus:host ratio 4 h after the onset of the light period and 100 ng ml^{-1} HHQ. Concurrent triplicate bottles were prepared with both viral lysate and a volumetric equivalent of DMSO. All treatments were incubated under general culturing conditions for 120 hpi.

Cultures were harvested daily for E. huxleyi cell counts, EhV enumeration, and a series of diagnostic fluorescent assays used to measure indicators of cell stress and PCD. Intracellular ROS production was measured by staining 200 μl of culture with 5 μM CM-H₂DCFDA for 90 min in the dark at 18°C. NO production was measured by staining 200 µl of culture with 5 μ M DAF-FM Diacetate dye for 45 min in the dark at 18°C. The concentration of dead cells was measured by staining 200 μ l of culture with 1 μ M of SYTOXTM Green dye for 10 min in the dark at 18°C. Membrane blebbing was measured by staining 200 μ l of culture with 10 μM of FM1-43FX dye for 30 min in the dark at 18°C. Lysosome presence was measured by staining 200 µl of culture with 1 µM of LysosensorTM Green DND-189 for 10 min in the dark at 18°C. All diagnostic fluorescent assays were read on the flow cytometer in 96-well plates with an excitation at 488 nm and emission at 512/18 nm. Fluorescent dye assays were prepared in the following order: ROS, NO, SYTOX, FM1-43FX, and Lysosome at each timepoint (0, 12, 24, 48, 72, 96 h).

For metacaspase assays, 25 ml cultures of exponential-phase *E. huxleyi* between 1 and 2×10^5

cells ml⁻¹ received one of 4 treatments in triplicate: DMSO only, 100 ng ml⁻¹ HHQ, EhV 201 + DMSO or EhV 201 + 100 ng ml⁻¹ HHQ. Cultures with virus were inoculated with a 1:1 virus:host ratio and cells were harvested daily for E. huxleyi cell counts and metacaspase activity until the viral-infected cultures dropped below 10³ cells ml⁻¹. Metacaspase activity was measured by staining 1 ml cultures with 20 μM CaspACE(TM) FITC-VAD-FMK dye for 20 min in the dark at 18°C. After staining, cells were washed once with 750 μ l of 1× PBS and concentrated on a 0.45 μ m nylon Spin-X column to a final volume of 400 μl. Concentrated samples were fixed in 2% formalin and stored in the dark at 4°C for up to 1 wk. Metacaspase activity was measured on the flow cytometer in 96well plates with an excitation at 488 nm and emission at 512/18 nm.

The lack of NO production observed in our initial round of diagnostic fluorescent assays prompted an additional examination of the impact of viral abundance and viral strain on NO production in DMSO-and HHQ-treated cultures. In triplicate 20 ml boro-

silicate tubes, $E.\ huxleyi$ cultures at a concentration of 1×10^5 cells ml⁻¹ were inoculated with viral lysate (EhV 86 or EhV 201) at either 8:1 or 1:1 virus:host ratio 4 h after the onset of the light period and 100 ng ml⁻¹ HHQ. Concurrent triplicate tubes were prepared with both viral lysate and a volumetric equivalent of DMSO. All treatments were incubated under general culturing conditions up to 120 h. NO production was measured with DAF-FM Diacetate dye as described above.

2.6. Statistical analyses

All statistical analyses were done using Prism 9 version 9.1.0 (GraphPad Software). Experiments that were conducted to examine changes in either *E. huxleyi* or virus abundance or *E. huxleyi* physiological activity over time were compared using a repeated-measures ANOVA with Sidak's multiple comparison post hoc tests. Growth rates were compared using a 1-way ANOVA, with Tukey's HSD post hoc analysis. Any p-values less than or equal to 0.05 were considered statistically significant for all tests.

3. RESULTS

Our previous work demonstrated that *Emiliania huxleyi* was protected from viral mortality when exposed to 100 ng ml⁻¹ HHQ (Pollara et al. 2021 and Fig. S1 in the Supplement at www.int-res.com/articles/suppl/a089p075_supp.pdf). Here, we demonstrate that this protection was only conferred when the alga was exposed to 100 ng ml⁻¹ of HHQ (Fig. 1a). Lower concentrations of HHQ (e.g. 1 and 10 ng ml⁻¹) resulted in *E. huxleyi* cell lysis by EhV 201; however, when cells were dosed at 100 ng ml⁻¹, both treatments exhibited static growth (i.e. no loss or gain of cell abundance). Based on these results, a dose of 100 ng ml⁻¹ HHQ was chosen as the concentration used in all subsequent experiments.

Protection against viral mortality was similar across 2 strains of EhV examined and varying ratios of virus to host tested (Fig. 1b). Similar to the dynamics observed with EhV 201, when *E. huxleyi* was exposed to EhV 86, cell abundance started to decline significantly at 48 hpi relative to DMSO control (p =

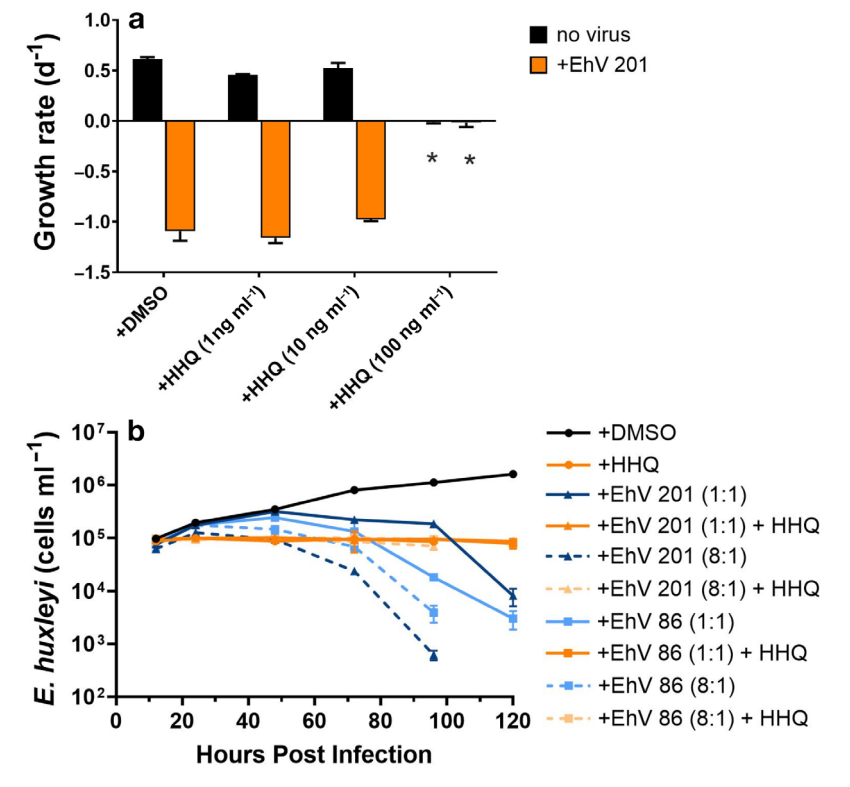


Fig. 1. (a) Growth rates of axenic *Emiliania huxleyi* in response to different concentrations of 2-heptyl-4-quinolone (HHQ) with and without *E. huxleyi* virus (EhV) 201 (1:1 virus: host ratio) over 96 h. Asterisks indicate a significant difference in growth rate from the +DMSO control. (b) Impact of 100 ng ml $^{-1}$ HHQ on the growth rate of *E. huxleyi* depending on viral strain (EhV 86 and EhV 201) and abundance. In both (a) and (b), means (\pm SD) are shown (n = 3); SD bars may be too small to visualize

0.02). A similar decline in abundance was not observed in *E. huxleyi* cells infected with EhV 86 and exposed to HHQ; rather, these cells maintained a static cell abundance throughout the experiment. Changing the virus-to-host ratio from 1:1 to 8:1 also did not alter the protection dynamics of HHQ but did influence how quickly viral mortality was induced. Higher virus-to-host ratios resulted in higher *E. huxleyi* cell losses irrespective of EhV strain used.

Pre-exposure assays provided an opportunity to evaluate the direct impact of HHQ on the infectivity of the virus. No significant difference in mortality was observed when *E. huxleyi* cells were infected with viral lysate, from either strain, pre-exposed to DMSO relative to HHQ (Fig. 2a,b). Moreover, pre-treating viral lysate with HHQ and then infecting *E.*

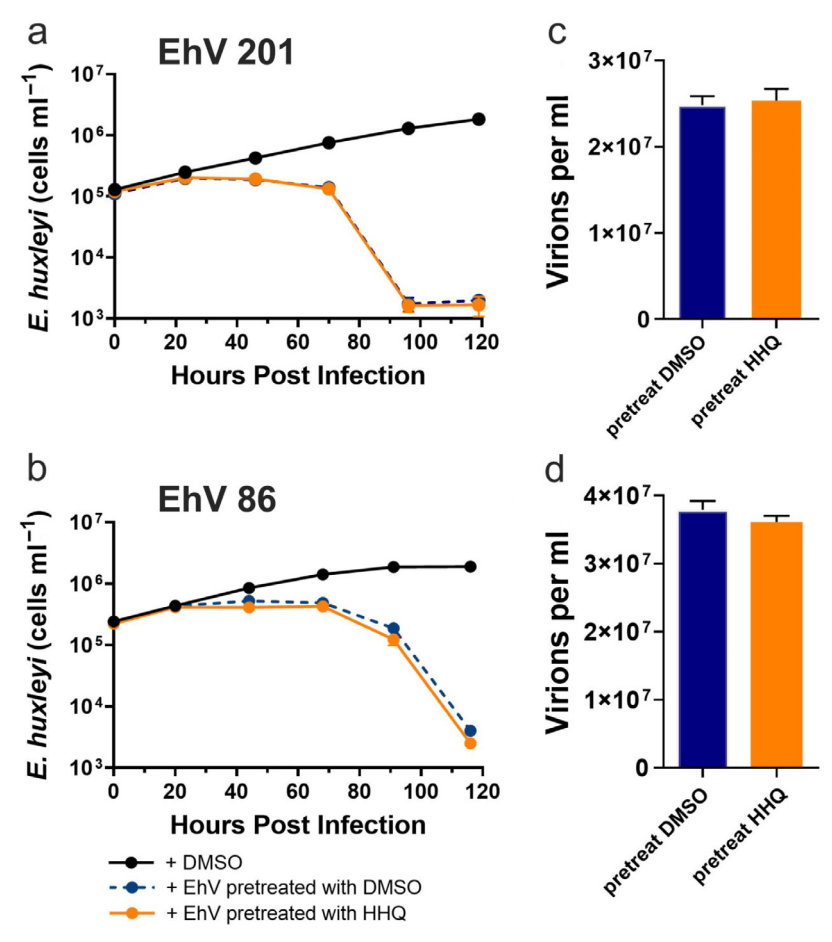


Fig. 2. Cell abundance was quantified from non-infected and infected cultures (1:1 virus: host ratio) where viral lysate from (a) EhV 201 and (b) EhV 86 was treated with 100 ng ml $^{-1}$ HHQ for 96 h prior to infection. Extracellular viral counts from (c) EhV 201 and (d) EhV 86 infected *E. huxleyi* cultures at 96 hpi (hours post infection) quantified by flow cytometry. No significant differences (p \leq 0.05) between extracellular viral abundances were observed at 96 hpi. For all treatments, means (\pm SD) are shown (n = 3); SD bars may be too small to visualize

huxleyi cells did not inhibit total viral production (Fig. 2c,d). Interestingly, HHQ did not confer protection of E. huxleyi if its addition was delayed to 24 hpi (p = 0.0002); however, delaying HHQ addition for 1 and 4 hpi did not inhibit viral lysis of E. huxleyi (Fig. S2). Based on these results, the remaining experiments were conducted by exposing E. huxleyi to virus and HHQ simultaneously at time zero.

TEM imaging showed that EhV 201 viral particles were present in infected *E. huxleyi* cells in both the presence and absence of HHQ (Fig. 3a–d). At 48 hpi, control cells treated only with EhV 201 exhibited viral particles enclosed in suspected early endosomes, as identified by the presence of membrane-bound vesicles (Fig. 3a,b). In contrast, EhV 201 + HHQ-treated cells showed cytoplasmic clearing and

endolysosomes formed upon the fusion of late endosomes and lysosomes, identified by the many intraluminal vesicles, membrane cargo, and enclosed granules with homogeneous electron density (Fig. 3c). Over the course of 72 h, there was no difference in the number of virions per cell in the presence and absence of 100 ng ml⁻¹ of HHQ (Fig. 3e). At 72 hpi, the percentage of cells that exhibited blebbing and compromised membranes in EhV 201 + HHQ-treated cells was reduced compared to cells exposed only to EhV 201 (Fig. S3a-d). Conversely, a larger percentage of cells were observed to have both thylakoid and cytoplasm lipid bodies in HHQ-exposed infected cells at 72 hpi compared to virus-only controls (Fig. S3a-d).

As viruses were able to gain entry into HHQ-exposed host cells, freevirion abundance upon viral release from the host was also examined. Total viral abundance peaked at 5.1×10^7 viruses ml⁻¹ at 72 hpi in the absence of HHQ, whereas total viral abundance did not exceed 1.0×10^6 viruses ml⁻¹ when the alga was exposed to HHQ (Fig. 4a). Beginning at 24 hpi, significant differences in total virus abundance between the DMSO and HHQ treatments were observed and continued through the end of the experiment (p = 0.002 or below). At time zero and 96 hpi, infectious viral

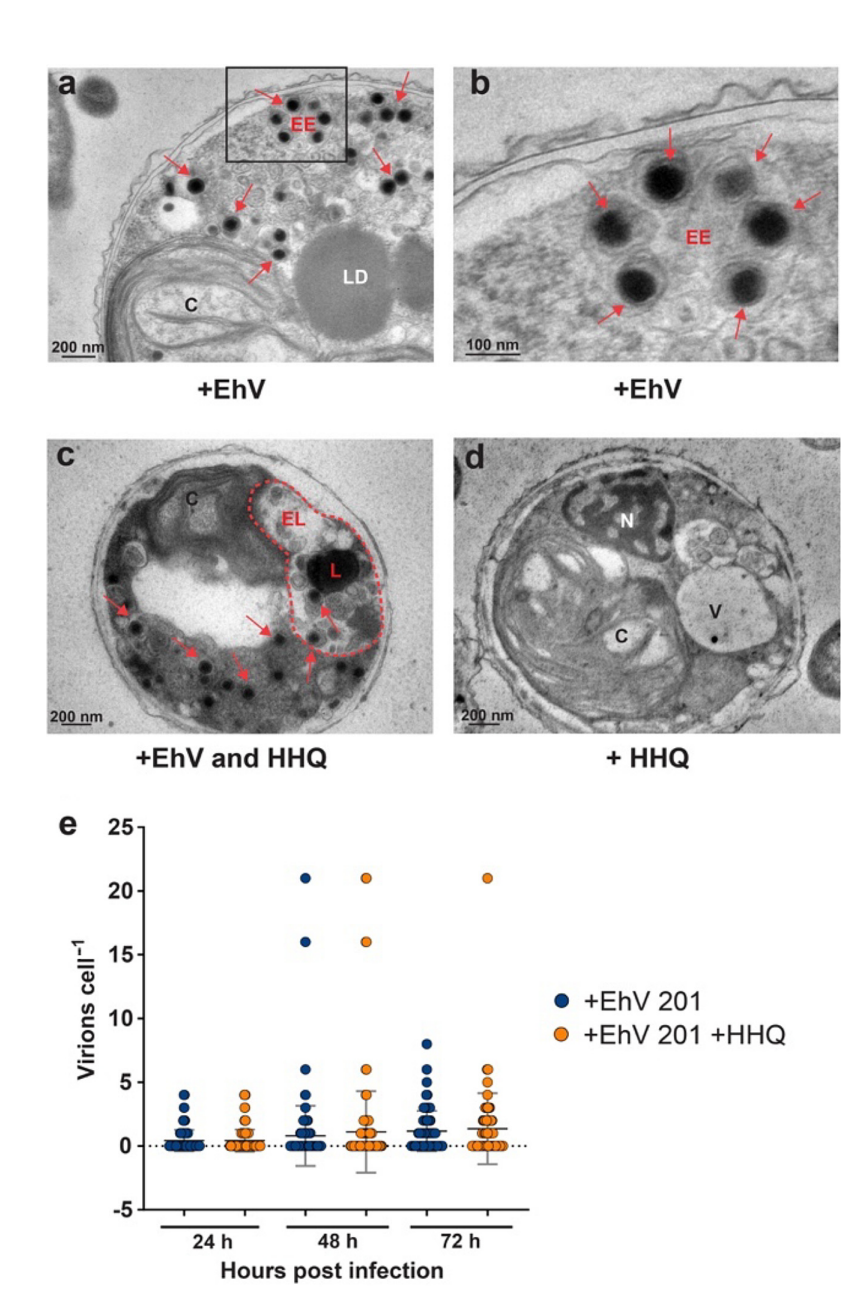


Fig. 3. Ultrastructure analysis of Emiliania huxleyi following infection with EhV 201 (8:1 virus:host ratio) in the presence and absence of HHQ. Representative transmission electron microscopy (TEM) images of E. huxleyi exposed to (a,b) EhV 201 only, (c) EhV 201 and 100 ng ml⁻¹ HHQ, or (d) 100 ng ml⁻¹ HHQ only at 48 hpi. EhV 201 virions were identified by an electron-dense core enveloped by a membrane. Early endosomes (EE, black box in a) were identified by membrane-bound vesicles. (b) Higher magnification of the boxed area depicting the early endosome in (a). Endolysosomes (EL, red dashed outline in c) were identified by the many intraluminal vesicles, membrane-bound cargo, and fused lysosomes (L) denoted by an electron-dense core with homogenous granularity. Arrows denote viral particles. Additional subcellular structures include the chloroplast (C), lipid droplet (LD), nucleus (N), and vacuole (V). Scale bars = 200 nm (a,c,d) and 100 nm (b). (e) Quantification of EhV 201 virions in E. huxleyi cells (n = 30 cells per treatment per time point) with and without HHQ imaged by TEM between 24 and 72 hpi. Mean ± SD is shown; no significant differences (p \leq 0.05) between intracellular viral abundances were observed in (e)

abundance was also enumerated. The abundance of infectious viruses increased several orders of magnitude over the course of the experiment, from 200 viruses ml⁻¹ at 0 h to 3.8×10^7 viruses ml⁻¹ at 96 hpi in infected cultures treated with DMSO (Fig. 4b). However, in the presence of HHQ, the abundance of infectious viruses only increased to approximately 1.8×10^4 active viruses ml⁻¹, 3 orders of magnitude lower than in the absence of HHQ. These results revealed a large disparity in the percent of active to total viruses, with approximately 62% of the total viruses being active in the absence of HHQ relative to only 1.3% in the presence of HHQ at 96 hpi. If we assume viral exit is due entirely to cell lysis, viral burst size from 48 to 96 hpi was different between the 2 treatments as well. When E. huxleyi was exposed only to EhV 201, burst size was 71 virions per host cell, compared to a burst size of 8.5 virions per host cell when E. huxleyi was exposed to both EhV 201 and HHQ.

Across all diagnostic stains tested, significant differences in cellular stress biomarkers were found between infected *E. huxleyi* cells in the presence and absence of HHQ (Fig. 5). In the absence of HHQ, the relative fluorescence of NO in E. huxleyi cells showed a rapid peak early in infection and then a rapid decline after 12 h (Fig. 5a). A similar peak was not observed when infected E. huxleyi cells were exposed to HHQ, with the relative fluorescence significantly lower (p < 0.001) than the DMSO control at all time points examined after 0 hpi. This pattern was observed irrespective of the strain of EhV used or virus:host ratio despite the magnitude of NO production scaling with virus:host ratio (Fig. S4). The percent of the infected *E. huxleyi* population stained for ROS was generally not significantly different when exposed to HHQ (Fig. 5b) outside of the 72 hpi time point (p = 0.021). Similarly, there was no significant difference in the

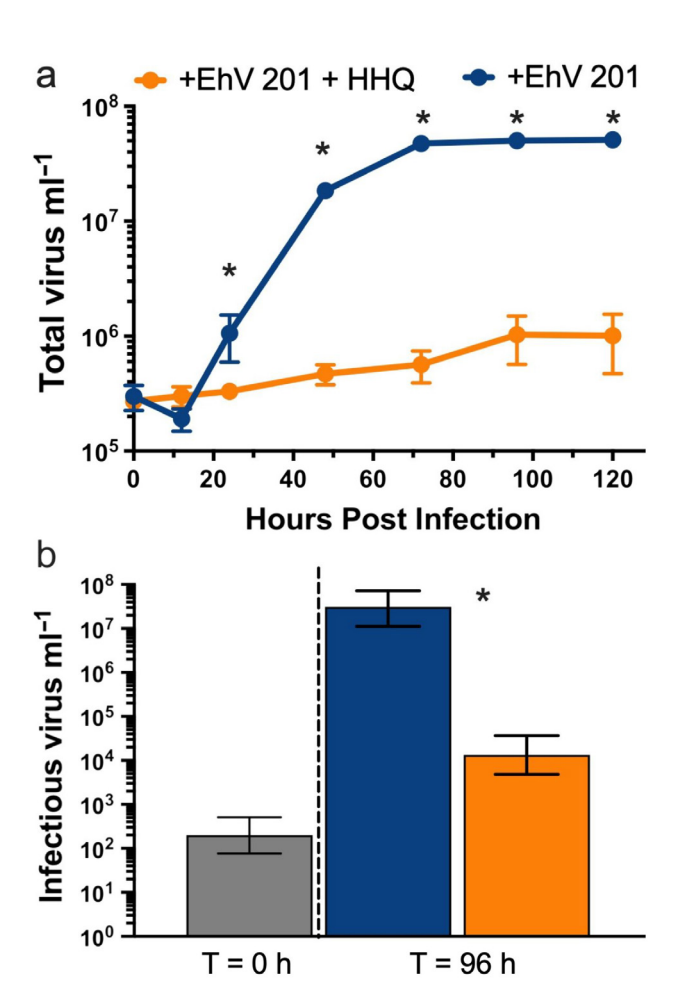


Fig. 4. Triplicate *Emiliania huxleyi* cultures were dosed simultaneously with EhV 201 (1:1 virus:host ratio) and 100 ng ml $^{-1}$ HHQ or EhV 201 alone, and the (a) abundance of extracellular viruses was measured every 24 h by flow cytometry over 120 hpi. (b) Total number of infectious or active viral particles was quantified using the most probable number assay at the start of the experiment (0 hpi) and at 96 hpi in both treatments. Mean \pm SD is shown. Asterisks indicate a significant difference (p \leq 0.05) in growth rate from the virus-only control

mean relative fluorescence between the 2 treatments for metacaspase over the course of the infection (Fig. 5c). For FM1-43FX (p = 0.002) and the population of SYTOX-activated cells (p = 0.0008), significantly lower signals were observed in infected $\it E. huxleyi$ cells in the presence of HHQ after 72 hpi (Fig. 5d–f).

4. DISCUSSION

Previous work demonstrated that *Emiliania huxleyi* exposure to the quorum sensing signal HHQ protected the algal host against viral lysis (Pollara et al.

2021); however, the mechanistic basis for this protection was unknown. The present study detailed the influence of HHQ on the efficacy of EhV infection in E. huxleyi and expands on the potential ecological role of bacterial chemical signals, like HHQ, in marine ecosystems. The concentration of HHQ found to inhibit viral-mediated cell lysis (100 ng ml⁻¹ or 410 nM) was also the observed growth inhibitory (IC₅₀) concentration for E. huxleyi strains (Harvey et al. 2016). Previous work also demonstrated that this IC_{50} concentration of HHQ had a significant impact on E. huxleyi morphology, physiology, and the transcriptomic and proteomic profiles of the alga, while exposure to HHQ concentrations < 100 ng ml⁻¹ had more minimal impacts (Pollara et al. 2021). Together, these findings indicate that a physiological restructuring of the alga at the IC₅₀ may play a critical role in viral protection. While the concentration of HHQ in situ in marine ecosystems is not well quantified (Pollara et al. 2021), it is unlikely that the few bulk measurements available accurately represent the effective HHQ concentration that an algal cell would experience in the phycosphere (Seymour et al. 2017, Shibl et al. 2020). Direct measurements of other metabolites (e.g. DMSP) in a microbial phycosphere indicated that concentrations were on the order of hundreds of mM, several orders of magnitude higher than the concentrations used here (Gao et al. 2020). Moreover, in situ measurements of HHQ concentrations produced by the human pathogen Pseudomonas aeruginosa range from 5 to 25 µM depending on stage of growth (Diggle et al. 2003), well above the IC₅₀ determined here (Harvey et al. 2016). Therefore, we hypothesize that 100 ng ml⁻¹ is both an ecologically relevant concentration of HHQ that could be obtained in the phycosphere by associated bacteria and a physiologically relevant concentration capable of influencing the success of viral dynamics in the field.

To examine if the effect of viral protection was mediated by direct interaction between EhV and HHQ, viral lysate was pretreated with HHQ for 96 h and then used to infect exponentially growing *E. huxleyi* cultures. No difference in viral infection dynamics was noted, including the trajectory of algal cell death and extracellular viral abundance 96 hpi, suggesting that HHQ does not degrade or influence EhVs directly. Rather, viral mortality evasion by HHQ is indirect, likely through the physiological alteration of the alga. Additionally, variability in the EhV strain did not alter the protection that HHQ afforded *E. huxleyi*. Comparison of EhV genomes has indicated significant differences in putative genes that influence the ecology and function of particular viral

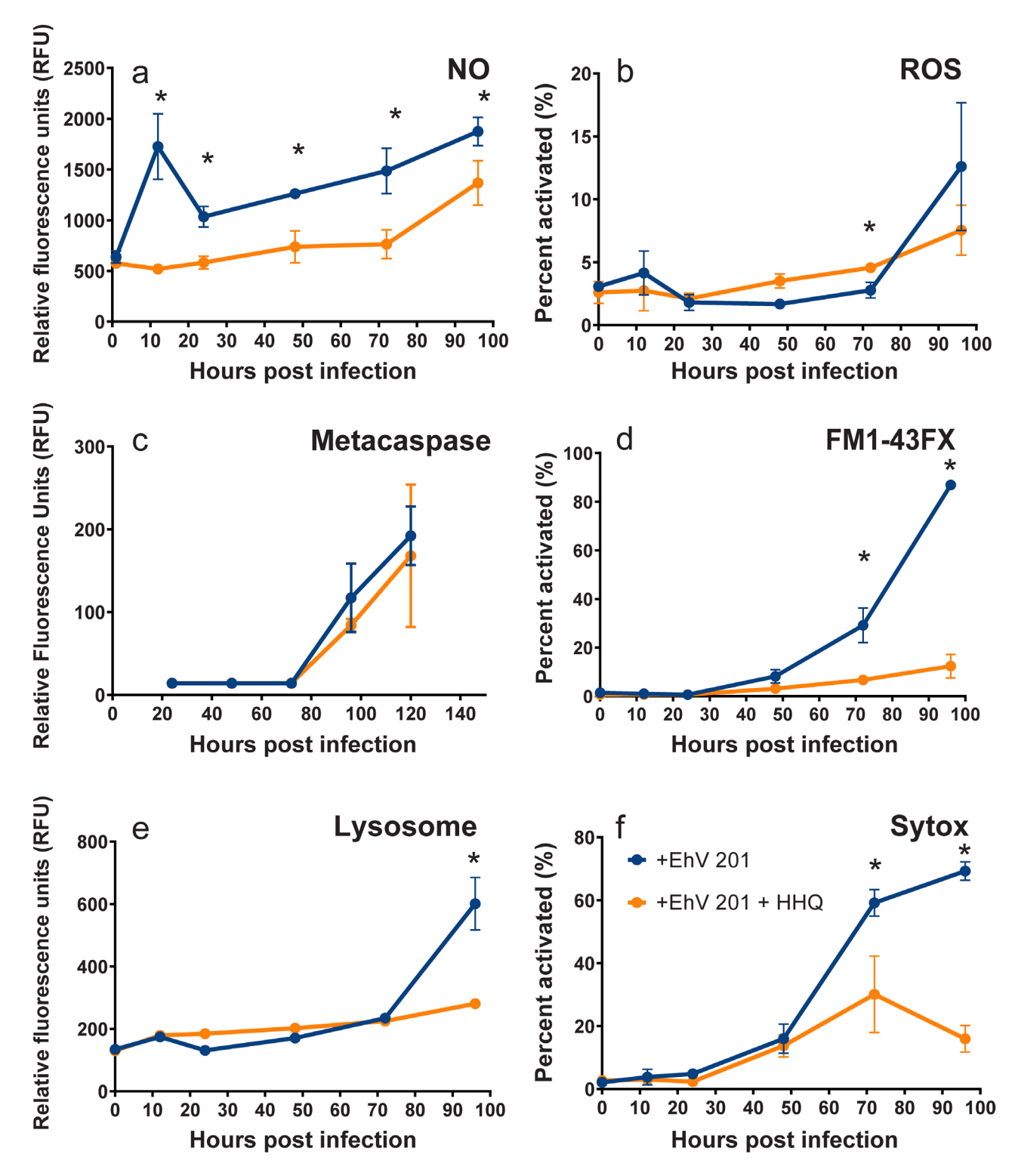


Fig. 5. Triplicate cultures of exponentially growing $Emiliania\ huxleyi\ cells$ were infected with EhV 201 at an 8:1 virus:host ratio (Fig. S1) and tracked for biochemical markers of cellular stress over the course of infection by flow cytometry. Infected cells were assessed for the presence of (a) intracellular reactive nitrogen species (NO) assessed by DAF-FM Diacetate dye, (b) intracellular reactive oxygen species (ROS) production measured by CM-H₂DCFDA, (c) intracellular metacaspase activation with CaspACE staining, (d) membrane blebbing using FM1-43FX, (e) detection of acidic compartments within cells using LysosensorTM Green DND-189, and (f) cell death assessed by SYTOX staining. Mean \pm SD is shown; asterisks indicate a significant difference (p \leq 0.05) in fluorescence staining from the virus-only control

strains (Nissimov et al. 2017), yet experiments herein suggest that HHQ-mediated protection against EhV was universal and triggered via fundamental changes within the algal host. Finally, the magnitude of the EhV inoculum dose did not alter HHQ-induced protection, indicating that the effects of HHQ are conferred independent of the encounter rate dynamics between EhV and host. Together, these findings continue to support the hypothesis that the influence of HHQ on the physiology of the host results in protection against viral infection.

Successful viral infection requires that the virus gain entry into, but also exit from, the host cell (Mackinder et al. 2009). TEM visualization of infected E. huxleyi cells clearly showed viral presence in HHQ-treated cells at 24 hpi with no significant difference in the number of virions per infected cell observed. It is hypothesized that EhVs gain entry into E. huxleyi using C-type lectins to attach, enter, and exit the cell via lipid rafts enriched with glycosphingolipids (Rose et al. 2014). Changes in the effectiveness of EhVs to gain entry into a host would be expressed in the percentage of the population exhibiting compromised membranes or membrane blebbing; however, no differences were observed in these parameters with exposure to HHQ, reinforcing the idea that HHQ does not prevent viruses from entering an E. huxleyi cell.

Results described here indicate that viral exit is compromised in HHQ-treated cells. In infected hosts exposed to HHQ, significantly fewer total extracellular viral particles were produced over the course of infection. Concomitantly, fewer infectious extracellular viruses were released, resulting in smaller calculated burst sizes. Various factors have been suggested to influence burst size, including nutrient content, temperature, and light (Raven 2006, Shemi et al. 2016, Thamatrakoln et al. 2019); however, the pool of available nucleotides needed for viral replication may ultimately constrain burst size (Brown et al. 2006). Select alkylquinolones are known to inhibit dihydroorotate dehydrogenase (DHODH), a key rate-limiting enzyme responsible for pyrimidine synthesis (Wu & Seyedsayamdost 2017). Moreover, inhibition of DHODH has been shown to decrease nucleotide pools, disrupt DNA replication, and accelerate genomic DNA lesions, thereby inducing intra-S-phase arrest in eukaryotes (Arnould et al. 2017, Fairus et al. 2017). HHQ-treated E. huxleyi exhibits an altered DNA damage response, including S-phase arrest (Pollara et al. 2021), which could drive the decrease in viral production observed. In addition, viral infection induces remodeling of the host lipidome whereby viral mem-

brane recruitment of recently released viruses become enriched in highly saturated triacylglycerols (TAGs) within 24 hpi in parallel with the formation of lipid droplets (Malitsky et al. 2016). An analysis of intact released virions demonstrates further enrichment of TAGs relative to host cells and indicates that viruses may exit (or bud) from the host via chemically distinct subcellular lipid microdomains, suggesting a physiological role for lipidome remodeling in enhancing viral infectivity and longevity in seawater (Malitsky et al. 2016). In HHQ-treated infected cells, there was significantly less membrane activity, as seen by the diagnostic fluorescent data FM1-43FX relative to EhVonly cells. Whether this disparity is due to reduced membrane blebbing or viral endo-/exocytosis cannot be determined from the present data. Furthermore, differences in the percentage of total lipid bodies in the cytoplasm observed in infected, HHQ-treated cells agree with results from previous work that found E. huxleyi exposure to HHQ induces cytoplasmic lipid droplet formation within 24 h of treatment in the alga (Pollara et al. 2021). What remains unknown is how the potential remodeling of lipid classes within the host due to HHQ exposure may impact viral exit or infectivity once released into the surrounding water. Together, these results indicate that viral replication and/or host cell exit strategy may be compromised in HHQ-treated E. huxleyi, accounting for the paucity in extracellular virus, decreased infectivity, and reduced burst size observed.

Finally, the ability of the virus to gain control of host PCD activation pathways is critical in preventing the host from activating PCD prematurely as a strategy to rid itself of the virus (Bidle & Falkowski 2004). During infection, EhVs actively manipulate host metabolism, hijack cellular autophagy processes (Schatz et al. 2014), induce the production of NO and ROS, in turn triggering metacaspase activity that induces PCD (Bidle et al. 2007, Vardi et al. 2012, Bidle 2015). Consequently, host susceptibility or resistance is thought to be mediated by the regulation of PCD machinery, which is an essential component of the viral replication strategy (Bidle 2016). Quantification of physiological activities using diagnostic fluorescent probes suggested PCD and cellular death were suppressed in infected E. huxleyi exposed to HHQ. One of the first stress signals heralding the onset of the lytic cycle in natural E. huxleyi populations due to the rapidity with which the signal interacts with cellular constituents is NO, a highly reactive gaseous free radical that can propagate quickly through phytoplankton populations leading to PCD activation (Bidle 2016). NO production occurs early in the trajectory of viral infection and does not occur simultaneously with ROS accumulation (Schieler et al. 2019). Here, we establish statistically significant differences in intracellular NO at 12 hpi, with DAF-FM Diacetate fluorescence being ~2- to 3-fold higher in infected cultures without HHQ. Moreover, NO induction was also dose-dependent conditional on viral load. In plant models, NO is a critical regulator of the proteolytic activity of metacaspases (Belenghi et al. 2007), and lower NO signaling early in lytic infection in HHQ-treated cells may indicate disruption of viral-mediated control of the PCD signaling pathway.

Together, these findings suggest that HHQ exposure stalls *E. huxleyi* mortality during viral infection by inhibiting viral replication/release and the activation of PCD pathways. This phenomenon is similar, regardless of EhV strain. Disruption of E. huxleyi mortality could allow cell-associated bacteria to continue to benefit from coordinated nutrient exchange, common between bacteria and phytoplankton (Cooper & Smith 2015). As has been demonstrated (Suttle 2007), viral lysis of *E. huxleyi* could shunt nutrients to the free-living or non-associated microbial assemblage at large, perhaps to the detriment of closely associated bacteria within the phycosphere. Additionally, viral infection of E. huxleyi can alter the metabolic profile of dissolved organic matter (DOM) (Kuhlisch et al. 2021), potentially producing DOM that is not desirable to closely phytoplankton-associated bacteria. Finally, viral infection of E. huxleyi has been implicated in enhancing carbon export through the stimulation of marine aggregates (Laber et al. 2018). Therefore, altering the trajectory of viral infection could directly alter carbon cycling on larger scales.

The consequence of the chemical crosstalk between phytoplankton and bacteria in shaping carbon and nutrient cycling represents the most significant inter-organism association in marine ecosystems. Collectively, these findings add a rich new layer of complexity to the viral–host story by presenting evidence for how bacterial communication signals provoke physiological remodeling of the algal host, resulting in viral resistance.

Acknowledgements. We thank Kay Bidle for sharing strains of *E. huxleyi* virus and Biao Zuo in the Electron Microscopy Resource Laboratory at the University of Pennsylvania for assistance with sample preparation. This work was funded by NSF grants (NSF OCE 1657818, 1657818; NSF IOS 2041748, 2041510) awarded to K.E.W. and E.L.H. E.L.H was also supported by a Sloan Foundation Research Fellowship. K.E.W was also supported by the Charles E. Kaufman Foundation Integrated Research Education Grant.

LITERATURE CITED

- Arnould S, Rodier G, Matar G, Vincent C and others (2017)
 Checkpoint kinase 1 inhibition sensitises transformed
 cells to dihydroorotate dehydrogenase inhibition. Oncotarget 8:95206–95222
- → Belenghi B, Romero-Puertas MC, Vercammen D, Brackenier
 A, Inzé D, Delledonne M, Breusegem FV (2007) Metacaspase activity of Arabidopsis thaliana is regulated by S-nitrosylation of a critical cysteine residue. J Biol Chem 282:1352–1358
- Bidle K (2015) The molecular ecophysiology of programmed cell death in marine phytoplankton. Annu Rev Mar Sci 7:341–375
- ∑Bidle KD (2016) Programmed cell death in unicellular phytoplankton. Curr Biol 26:R594−R607
- Bidle KD, Falkowski PG (2004) Cell death in planktonic, photosynthetic microorganisms. Nat Rev Microbiol 2:643–655
- → Bidle KD, Vardi A (2011) A chemical arms race at sea mediates algal host-virus interactions. Curr Opin Microbiol 14:449-457
- Fratbak G, Egge JK, Heldal M (1993) Viral mortality of the marine alga *Emiliania huxleyi* (Haptophyceae) and termination of algal blooms. Mar Ecol Prog Ser 93:39–48
- Brown CM, Lawrence JE, Campbell DA (2006) Are phytoplankton population density maxima predictable through analysis of host and viral genomic DNA content? J Mar Biol Assoc UK 86:491–498
- Cooper MB, Smith AG (2015) Exploring mutualistic interactions between microalgae and bacteria in the omics age. Curr Opin Plant Biol 26:147–153
- Diggle SP, Winzer K, Chhabra SR, Worrall KE, Cámara M, Williams P (2003) The *Pseudomonas aeruginosa* quinolone signal molecule overcomes the cell density-dependency of the quorum sensing hierarchy, regulates *rhl*-dependent genes at the onset of stationary phase and can be produced in the absence of LasR. Mol Microbiol 50:29–43
- Fairus AKM, Choudhary B, Hosahalli S, Kavitha N, Shatrah O (2017) Dihydroorotate dehydrogenase (DHODH) inhibitors affect ATP depletion, endogenous ROS and mediate S-phase arrest in breast cancer cells. Biochimie 135:154–163
- Frada MJ, Rosenwasser S, Ben-Dor S, Shemi A, Sabanay H, Vardi A (2017) Morphological switch to a resistant subpopulation in response to viral infection in the bloomforming coccolithophore *Emiliania huxleyi*. PLOS Pathog 13:e1006775
- Gao C, Fernandez VI, Lee KS, Fenizia S and others (2020) Single-cell bacterial transcription measurements reveal the importance of dimethylsulfoniopropionate (DMSP) hotspots in ocean sulfur cycling. Nat Commun 11:1942
 - Guillard RRL (1975) Culture of phytoplankton for feeding marine invertebrates. In: Smith WL, Chanley MH (eds) Culture of marine invertebrate animals: proceedings—

 1st conference on culture of marine invertebrate animals

 Greenport. Springer, Boston, MA, p 29–60
- *Harvey EL, Deering RW, Rowley DC, El Gamal A and others (2016) A bacterial quorum sensing precursor induces mortality in the marine coccolithophore, *Emiliania huxleyi*. Front Microbiol 7:59

- Holligan PM, Fernández E, Aiken J, Balch WM and others (1993) A biogeochemical study of the coccolithophore, *Emiliania huxleyi*, in the North Atlantic. Global Biogeochem Cycles 7:879–900
- Jacquet S, Heldal M, Iglesias-Rodriguez D, Larsen A, Wilson W, Bratbak G (2002) Flow cytometric analysis of an *Emiliania huxleyi* bloom terminated by viral infection. Aquat Microb Ecol 27:111–124
- Jarvis B, Wilrich C, Wilrich P (2010) Reconsideration of the derivation of Most Probable Numbers, their standard deviations, confidence bounds and rarity values. J Appl Microbiol 109:1660–1667
- Kendrick BJ, DiTullio GR, Cyronak TJ, Fulton JM, Mooy BASV, Bidle KD (2014) Temperature-induced viral resistance in *Emiliania huxleyi* (Prymnesiophyceae). PLOS ONE 9:e112134
- Knowles B, Bonachela JA, Behrenfeld MJ, Bondoc KG and others (2020) Temperate infection in a virus-host system previously known for virulent dynamics. Nat Commun 11:4626
- Ku C, Sheyn U, Sebe-Pedros A, Ben-Dor S and others (2020) A single-cell view on algal-virus interactions reveals sequential transcriptional programs and infection states. Sci Adv 6:eaba4137
- Kuhlisch C, Schleyer G, Shahaf N, Vincent F, Schatz D, Vardi A (2021) Viral infection of algal blooms leaves a unique metabolic footprint on the dissolved organic matter in the ocean. Sci Adv 7:eabf4680
- Laber CP, Hunter JE, Carvalho F, Collins JR and others (2018) Coccolithovirus facilitation of carbon export in the North Atlantic. Nat Microbiol 3:537–547
- Liu J, Cai W, Fang X, Wang X, Li G (2018) Virus-induced apoptosis and phosphorylation form of metacaspase in the marine coccolithophorid *Emiliania huxleyi*. Arch Microbiol 200:413–422
- Mackinder LCM, Worthy CA, Biggi G, Hall M and others (2009) A unicellular algal virus, *Emiliania huxleyi* virus 86, exploits an animal-like infection strategy. J Gen Virol 90:2306–2316
- Malitsky S, Ziv C, Rosenwasser S, Zheng S and others (2016) Viral infection of the marine alga *Emiliania huxleyi* triggers lipidome remodeling and induces the production of highly saturated triacylglycerol. New Phytol 210:88–96
- Nissimov JI, Worthy CA, Rooks P, Napier JA and others (2012) Draft genome sequence of the coccolithovirus Emiliania huxleyi virus 202. J Virol 86:2380–2381
- Nissimov J, Pagaret A, Ma F, Cody S, Dunigan D, Kimmance S, Allen M (2017) Coccolithoviruses: a review of crosskingdom genomic thievery and metabolic thuggery. Viruses 52:v9030052
- Paasche E (2001) A review of the coccolithophorid *Emiliania* huxleyi (Prymnesiophyceae), with particular reference to growth, coccolith formation, and calcification–photosynthesis interactions. Phycologia 40:503–529
- Pollara SB, Becker JW, Nunn BL, Boiteau R and others (2021) Bacterial quorum sensing signal arrests phytoplankton cell division and impacts virus-induced mortality. MSphere 6:e00009–e00021
- Raven JA (2006) Aquatic viruses: the emerging story. J Mar Biol Assoc UK 86:449–451
- 🔭 Read BA, Kegel J, Klute MJ, Kuo A and others (2013) Pan

- genome of the phytoplankton *Emiliania* underpins its global distribution. Nature 499:209–213
- Rose SL, Fulton JM, Brown CM, Natale F, Van Mooy BAS, Bidle KD (2014) Isolation and characterization of lipid rafts in *Emiliania huxleyi*: a role for membrane microdomains in host-virus interactions. Environ Microbiol 16:1150-1166
- Rosenwasser S, Mausz MA, Schatz D, Sheyn U and others (2014) Rewiring host lipid metabolism by large viruses determines the fate of *Emiliania huxleyi*, a bloom-forming alga in the ocean. Plant Cell 26:2689–2707
- Schatz D, Shemi A, Rosenwasser S, Sabanay H, Wolf S, Ben-Dor S, Vardi A (2014) Hijacking of an autophagy-like process is critical for the life cycle of a DNA virus infecting oceanic algal blooms. New Phytol 204:854–863
- Schatz D, Schleyer G, Saltvedt MR, Sandaa RA, Feldmesser E, Vardi A (2021) Ecological significance of extracellular vesicles in modulating host-virus interactions during algal blooms. ISME J 15:3714-3721
- Schieler BM, Soni MV, Brown CM, Coolen MJL and others (2019) Nitric oxide production and antioxidant function during viral infection of the coccolithophore *Emiliania huxleyi*. ISME J 13:1019–1031
- Schindelin J, Arganda-Carreras I, Frise E, Kaynig V and others (2012) Fiji: an open-source platform for biological-image analysis. Nat Methods 9:676–682
- Seymour JR, Amin SA, Raina JB, Stocker R (2017) Zooming in on the phycosphere: the ecological interface for phytoplankton-bacteria relationships. Nat Microbiol 2:1-12
- Shemi A, Schatz D, Fredricks HF, Van Mooy BAS, Porat Z, Vardi A (2016) Phosphorus starvation induces membrane remodeling and recycling in *Emiliania huxleyi*. New Phytol 211:886–898
- Shibl AA, Isaac A, Ochsenkuhn MA, Cárdenas A and others (2020) Diatom modulation of select bacteria through use of two unique secondary metabolites. Proc Natl Acad Sci USA 117:27445–27455
- Suttle CA (2005) Viruses in the sea. Nature 437:356–361
- Suttle CA (2007) Marine viruses major players in the global ecosystem. Nat Rev Microbiol 5:801–812
- Thamatrakoln K, Talmy D, Haramaty L, Maniscalco C and others (2019) Light regulation of coccolithophore hostvirus interactions. New Phytol 221:1289–1302
- Vardi A, Haramaty L, Van Mooy BAS, Fredricks HF, Kimmance SA, Larsen A, Bidle KD (2012) Host-virus dynamics and subcellular controls of cell fate in a natural coccolithophore population. Proc Natl Acad Sci USA 109: 19327-19332
- Wilson W, Tarran G, Schroeder D, Cox M, Oke J, Malin G (2002) Isolation of viruses responsible for the demise of an *Emiliania huxleyi* bloom in the English Channel. J Mar Biol Assoc UK 82:369–377
- Wu Y, Seyedsayamdost MR (2017) Synergy and target promiscuity drive structural divergence in bacterial alkylquinolone biosynthesis. Cell Chem Biol 24:1437–1444.e3
- Zhang E, Gao J, Wei Z, Zeng J, Li J, Li G, Liu J (2022) MicroRNA-mediated regulation of lipid metabolism in virus-infected *Emiliania huxleyi*. ISME J 16:2457–2466
- Zondervan I, Rost B, Riebesell U (2002) Effect of CO₂ concentration on the PIC/POC ratio in the coccolithophore *Emiliania huxleyi* grown under light-limiting conditions and different daylengths. J Exp Mar Biol Ecol 272:55–70